Oxidative stress increases eukaryotic initiation factor 4E phosphorylation in vascular cells

Roger F. DUNCAN*†[1], Hazel PETERSON*, Curt H. HAGEDORN‡ and Alex SEVANIAN*

*Department of Molecular Pharmacology and Toxicology, School of Pharmacy, University of Southern California, 1985 Zonal Avenue, Los Angeles, CA 90033, U.S.A., †Department of Molecular Microbiology and Immunology, School of Medicine, University of Southern California, 2011 Zonal Avenue, Los Angeles, CA 90033, U.S.A., and ‡Department of Medicine, Emory University School of Medicine, 165 Michael Street, Atlanta, GA 30322, U.S.A.

Dysregulated cell growth can be caused by increased activity of protein synthesis eukaryotic initiation factor (eIF) 4E. Dysregulated cell growth is also characteristic of atherosclerosis. It is postulated that exposure of vascular cells, such as endothelial cells, smooth muscle cells and monocytes/macrophages, to oxidants, such as oxidized low-density lipoprotein (oxLDL), leads to the elaboration of growth factors and cytokines, which in turn results in smooth muscle cell hyperproliferation. To investigate whether activation of eIF4E might play a role in this hyperproliferative response, vascular cells were treated with oxLDL, oxidized lipid components of oxLDL and several model oxidants, including H_2O_2 and dimethyl naphthoquinone. Exposure to each of these compounds led to a dose- and time-dependent increase in eIF4E phosphorylation in all three types of vascular cells, correlated with a modest increase in overall translation rate. No changes in eIF4EBP, eIF2 or eIF4B modification state were observed. Increased eIF4E phosphorylation was paralleled by increased presence of eIF4E in high-molecular-mass protein complexes characteristic of its most active form. Anti-oxidants at concentrations typically employed to block oxidant-induced cell signalling likewise promoted eIF4E phosphorylation. The results of this study indicate that increased eIF4E activity may contribute to the pathophysiological events in early atherogenesis by increasing the expression of translationally inefficient mRNAs encoding growth-promoting proteins.

Key words: initiation factors, oxidative stress, phosphorylation, protein synthesis.

INTRODUCTION

Numerous pathophysiological situations, including early atherogenesis, are characterized by dysregulated cell growth (e.g. [1,2]). In many cases, specific and inappropriate proto-oncogene expression occurs [1,2]. Totally unregulated cell growth (carcinogenesis) represents the extreme case, but in other instances hyperplasia is sufficient to cause a pathophysiological state. In this study, we have focused on the excessive growth of vascular cells associated with the formation of atherosclerotic plaques, and the molecular mechanism(s) underlying hyperproliferation.

A prominent hypothesis suggests that oxidative stress is an initiator stimulus in atherogenesis [3–5], as well as many other pathophysiologic situations, such as skin cancer and arthritis. Atherogenesis may result from the intravasion of low-density lipoprotein (LDL) particles into the vessel intima, followed by the cell-mediated oxidation of LDL to oxidatively-modified LDL [5], perhaps exacerbated by inflammatory reactions initiated at the lumen–endothelium interface. Several lines of evidence support this model. Lipid oxidation products are associated with atherosclerotic lesions, oxidized LDL (oxLDL) generates atherogenic-associated effects in *in vitro* studies, and antioxidants prevent atherogenesis in animal models (reviewed in [5]). oxLDL activates transcription in vascular cells to increase their production of cytokines and growth factors capable of initiating a hyperplastic response. These factors include interleukin 1β, interleukin-6, tumour necrosis factor-α (TNF-α), monocyte chemotactic protein-1 ('MCP-1'), platelet-derived growth factor (PDGF), basic fibroblast growth factor (bFGF), heparin-binding epidermal growth factor-like growth factor ('HB-EGF'), granulocyte/macrophage colony-stimulating factor ('GM-CSF'), and macrophage colony stimulating factor ('M-CSF') (reviewed in [1,2,5]).

Many of these transcriptionally induced mRNAs contain high extents of secondary structure in their 5′ untranslated regions (5′UTRs) that have been shown or predicted to severely repress their translation (e.g. PDGF [6], c-*myc* [7] and bFGF [8] mRNAs; similar effects have been shown for model structure-burdened mRNAs [9]). Therefore, the transcriptional induction of these genes may not be sufficient to account for their increased protein production by vascular cells following oxLDL stress.

It has been clearly established that increased eukaryotic initiation factor (eIF) 4E activity can enhance the translation of 5′UTR secondary structure-burdened mRNAs [10–12]. There-

Abbreviations used: AMLYS, ampholine lysis buffer; bFGF, basic fibroblast growth factor; BHA, butylated hydroxyanisole; BHT, butylated hydroxytoluene; DCF, 2′,7′-dichlorofluorescein; 1DGE, one-dimensional SDS gel electrophoresis as described by Laemmli; 2DGE, two-dimensional gel electrophoresis, using IEF in the first dimension and 1DGE in the second dimension; DMEM, Dulbecco's minimal essential medium; DMNQ, dimethyl naphthoquinone; eIF, eukaryotic initiation factor; ERK, extracellular signal-related kinase; GLB, Garrell's lysis buffer; IEF, isoelectric focusing; LDL, low-density lipoprotein; LOOH, linoleic acid hydroperoxide; MAP kinase, mitogen-activated protein kinase; MNK1, MAP kinase signal-integrating kinase; NAC, *N*-acetylcysteine; NF-κB, nuclear factor κB; oxLDL, oxidized LDL; PDGF, platelet-derived growth factor; PDTC, 1-pyrrolidinecarbodithioic acid; rpS6, ribosomal protein S6; ROS, reactive oxygen species; SMC, smooth muscle cells; tLDL, total LDL; TNF-α, tumour necrosis factor α; 5′UTR, 5′ untranslated region.

[1] To whom correspondence should be addressed (e-mail rduncan@hsc.usc.edu).

fore, we hypothesized that increased eIF4E activity might be a required feature of proto-oncogene expression-mediated early atherogenic events. A translational regulation component to atherogenesis has not, as yet, been addressed. Considering that several of the oxLDL-induced mRNAs have burdened 5′UTRs, there would be a 'metabolic logic' to the parallel activation of the translation 'unwinding machinery' mediated by eIF4E.

Protein synthesis eIF4E plays a critical role in regulating overall translation rate, the types of proteins being synthesized, and cell growth rate [13]. eIF4E, in combination with eIF4A and eIF4G, constitute the heterotrimeric protein synthesis eIF4F. The eIF4E subunit specifically binds to the 5′ m^{7}GpppG cap structure of mRNA, which concurrently or subsequently recruits eIF4G/4A and eIF3, ultimately creating an 'open' cap-proximal mRNA region capable of binding the 43S ribosome subunit complex. High amounts of 5′UTR secondary structure sterically restrict ribosome binding and scanning, and thereby inhibit mRNA translation [14].

eIF4E activity is regulated by its abundance, by its phosphorylation state, and by eIF4E-binding proteins [13]. Deregulating its activity through overexpression (increased abundance) results in anchorage-independent cell growth, overall faster cell division, and the ability to form tumours in nude mice [15], as well as aberrant growth and mitotic abnormalities in HeLa cells [16]. Overexpressed eIF4E co-operates with c-*myc* to cause transformation of primary cells as efficiently as oncogenic *ras* mutants [17]. Conversely, antisense-mediated reduced abundance blocks *ras*-induced cell transformation, decreases cell division rate [18,19], and favours translation of mRNAs (e.g. heat shock protein mRNAs) with minimal 5′UTR secondary structure [20].

Cell transformation caused by eIF4E overexpression requires the increased translation of several mRNAs encoding key growth regulatory proteins, whose expression is normally limited by inefficient translation, due, at least in part, to high secondary structure in their 5′UTRs [9]. For example, ornithine decarboxylase mRNA is translationally activated in response to eIF4E overexpression, and specifically blocking eIF4E-induced increased synthesis reverses the transformed phenotype [11]. Other proto-oncogene mRNAs activated by eIF4E overexpression include cyclin D1, bFGF (also called FGF-2), and c-*myc* [10,12,21].

eIF4E activity is also regulated by its phosphorylation state. Most stimuli which activate the translational machinery increase eIF4E phosphorylation, and most translation repressing situations result in its dephosphorylation [22]. A simple model suggesting phosphorylation increases the binding of eIF4E to mRNA has been called into question by recent results. A careful examination of the effect of phosphorylation on eIF4E binding to capped mRNA indicates affinity is reduced approx. 10-fold [23], contrary to a previous report of a several-fold increase in affinity [24]. Identification of serine-209 as the principal phosphorylation site [25,26] suggested that increased affinity for mRNA could result from the formation a 'restraining collar' around the eIF4E-bound mRNA via a salt bridge with a proximal lysine (K159) [27], but this model is not supported by the *in vitro* direct binding measurements. However, phosphorylated eIF4E predominates in the eIF4F complex [28], the most active form of eIF4E [29], and in 48S initiation complexes [30], and phosphorylation is required for normal development [31]. A specific influence of eIF4E phosphorylation on proto-oncogene mRNA translation has not been elucidated as yet.

In this study we have investigated the effects of oxidative stress, caused by oxLDL, oxidized components of LDL and model oxidant compounds, on eIF4E in cells of the vasculature, such as endothelial cells, smooth muscle cells (SMCs), and macrophages. We find that these compounds potently increase eIF4E phosphorylation (though not its abundance) and activity, defining a critical new component of the vascular oxidative stress response with links to cell hypertrophy. Together, these results implicate translational control of gene expression mediated by eIF4E in atherogenesis, as elaborated in the Discussion section.

EXPERIMENTAL

Materials

m^{7}GTP-Sepharose and ampholines were purchased from Amersham Pharmacia (Piscataway, NJ, U.S.A.). Sepharose CL-6B, RNase A and T1, benzamidine, aprotinin, PMSF, butylated hydroxytoluene (BHT), butylated hydroxyanisole (BHA), lipoic acid, *N*-acetylcysteine, pyrrolidine dithiocarbamate, hydrogen peroxide, glucose oxidase, glucose, catalase, TNF-α, PMA, anisomycin and amphotericin/penicillin/streptomycin antibiotic mix were purchased from Sigma Chemical Co. (St. Louis, MO, U.S.A.). Acrylamide and Triton X-100 were purchased from Serva (Heidelberg, Germany). Urea (biotechnology grade) was purchased from Fisher Scientific (Pittsburgh, PA, U.S.A.). Chemiluminescence detection reagents were purchased from Kierkegard and Perry Laboratories (KPL, Gaithersburg, MD, U.S.A.). HYPERfilm was purchased from Amersham Pharmacia. Immobilon P PVDF membrane was purchased from Millipore (Bedford, MA, U.S.A.). [^{35}S]Methionine and [^{3}H]-thymidine were purchased from ICN (Irvine, CA, U.S.A.). Dimethyl naphthoquinone (DMNQ) and menadione were provided by Dr H. J. Forman (Department of Environmental Health Sciences, School of Public Health and Center for Free Radical Biology, University of Alabama, AL, U.S.A.). Linoleic acid hydroperoxide (LOOH) was prepared as described previously [32].

Lipoprotein and LDL isolation

Unmodified LDL and LDL were prepared as described previously [33]. Briefly, venous blood from healthy volunteers was collected into vacutainer tubes, and plasma was immediately separated by centrifugation at 1500 ***g*** for 10 min at 4 °C, and 1 mM PMSF, 2 mM benzamidine, 2 mg/ml aprotinin and 20 mM BHT were added to prevent protease activity and oxidative reactions. LDL ($1.019 < d < 1.063$ g/ml) was isolated from freshly drawn plasma by preparative ultracentrifugation (5 h at 30000 ***g***) (Sorvall Ultra Pro80) using a vertical rotor (T-1270) at 4 °C. After separation, the LDL was dialysed against 150 mM NaCl, 1 mM EDTA, 10 mM Trizma base and 3.0 mM sodium azide at 4 °C for 12 h.

To separate total plasma LDL into the unmodified LDL and electronegative LDL subfractions, samples were adjusted to a final concentration of 1.0 mg of protein/ml of LDL and separated by ion exchange-HPLC monitored at 280 nm (Shimadzu, Kyoto, Japan), using a 7.0 mm × 35.0 mm UNO Q-1 column (Bio-Rad, Hercules, CA, U.S.A). A 1 ml sample was injected and eluted at 1.0 ml/min with helium-spared and pressurized 0.01M Tris/HCl (pH 7.2) starting buffer. After 5 min, a 0–0.3 M NaCl gradient in Tris/HCl buffer was eluted over the remaining 45 min. The peaks were collected in tubes containing 1 mg/ml EDTA, 1 mM PMSF, 2 mM benzamidine, 2 mg/ml aprotinin and 20 mM BHT that were immersed in an ice bath. Lipoproteins were concentrated using a Speed-Vac SC 110 (Savant Instruments, Holbrook, NY, U.S.A.) and salts were removed using Econo-Pac 10DG columns (Bio-Rad). Immunoglobulins and albumin were eliminated with an Econo-Pac Serum IgG purification kit (Bio-Rad). Charac-

Table 1 Composition of native LDL (nLDL) and naturally oxidized, more electronegative LDL (LDL−)

nLDL and LDL− were purified from total lipoproteins by HPLC, as described in the Experimental section. Purified samples were characterized for the mole ratios of the following components relative to apolipoprotein B (1 molecule per particle of LDL): α-tocopherol, PUFA (polyunsaturated fatty acids), dienes, LOOH, LPC (lysophosphatidylcholine), MDA (malondialdehyde) and MDA adducts. REM, mobility on agarose gel electrophoresis relative to nLDL.

Component	mol/mol LDL in nLDL	mol/mol LDL in LDL−
α-Tocopherol	6.4	2–6
PUFA	1300	910
Dienes	3	10
LOOH	3	7
LPC	80	140
MDA	2	7.3
MDA adducts	0.0096	0.016
REM	1	1.2

teristics of the non-modified LDL and electronegative LDL are listed in Table 1.

Lysate preparation

Cells were routinely propagated in 6-well culture dishes to 75–95% confluence. Rabbit endothelial cells and SMCs were obtained from New Zealand White rabbits, and used between passages 13–20. J774 macrophages were obtained from the American Type Culture Collection. Cells were propagated as described previously [34]. Treatments with oxLDL were carried out by removing the medium from the wells, washing 1–3 times with Dulbecco's minimal essential medium (DMEM), then adding DMEM containing 0.5% LDL-deficient serum with or without LDL. Treatments with LOOH or H_2O_2 were carried out as described above, except the wash and treatment buffer was PBS. The removed growth medium was saved and after 15 min, the peroxide-containing PBS was aspirated and the reserved growth media were returned to the wells. DMNQ and menadione were added directly to the growth medium. Lysates were prepared from 1 well, yielding 100–200 μg of protein, by washing the wells 1–2 times with Earle's Buffered Salts Solution (EBSS), scraping the cells in 2 ml of EBSS, pelleting for 50 s at approx. 1750 ***g*** in a clinical centrifuge (IEC, Needham Heights, MA, U.S.A.), then adding 100–200 μl of GLB (Garrell's lysis buffer) [0.3% (w/v) SDS buffer, 50 mM Tris pH 8.0, 1% 2-mercaptoethanol] for one-dimensional gel analyses, or AMLYS (ampholine lysis buffer) {9.8 M urea, 2% (v/v) Triton X-100, 0.5% 3–10 ampholines (Bio-Rad), 0.1% 2-mercaptoethanol [35]} for two-dimensional gel analysis. The pellet was disrupted by pipetting. For GLB lysates, 1/20 of the volume of RNase/DNase solution [5 mg/ml DNAse, 2.5 mg/ml RNase A, 500 mM Tris (pH 7.0) and 50 mM $MgCl_2$) was added for approx. 1 min, the viscosity reduced by pipetting, and then urea was added at 100 mg/100 μl of lysate.

Electrophoresis and immunoblotting

Two-dimensional isoelectric focusing (IEF)/SDS/PAGE was performed basically as described previously [35]. The first dimension used 80% pH range 5–7 and 20% pH range 3.5–10 ampholines (Amersham Pharmacia or Bio-Rad); the second dimension gels were 10.5% acrylamide, except for the eIF4E-BP1 (also called PHAS-I) analysis, which used 100% pH range 3.5–10 ampholines (Bio-Rad) in the first dimension and 11.5% acrylamide in the second dimension. One-dimensional gel analysis was performed identically with the second dimension step of IEF/SDS/PAGE. Gels were transferred on to ImmobilonP (Millipore) at 300 mA for 3 h in a liquid transfer tank (Amersham Pharmacia) using Laemmli formulation SDS/PAGE running gel tank buffer with SDS reduced to 0.01% (w/v) and methanol added to 15% (v/v). Gels were stained with 0.1% (w/v) Amido Schwartz in destaining solution [80% (v/v) methanol, 2% (v/v) acetic acid] for approx. 5 min, destained with 2 rinses of destaining solution, and pre-blocked with 5% non-fat milk in TBS [20 mM Tris HCl (pH 7.6), 137 mM NaCl] for 30 min at 22–24 °C on a rocker table. Subsequent chemiluminescence detection using Hyperfilm was performed according to manufacturer's instructions (ECL® Western blotting kit, Amersham Pharmacia). First antibody was used at 1:5000 dilution for 2 h with rocking at 22–24 °C in small plastic boxes. Second antibody was used at 1:30000 dilution for 1 h. Protein spots were quantified by densitometry using the BioImage system (Millipore).

Sepharose CL-6B column chromatography

Lysates were prepared from a 100 mm tissue culture dish of 75–95% confluent cells, untreated or treated. Cells were washed 3 times on the dish with EBSS, then scraped in 5 ml of EBSS and pelleted in the clinical centrifuge as described above. The cell pellets were resuspended in 250 μl of 4 °C m^7GTP column buffer [100 mM KCl, 20 mM HEPES (pH 7.6), 7 mM 2-mercaptoethanol, 0.2 mM EDTA, 10% (w/v) glycerol] to which the following components were added for lysis: Triton X-100 to 0.1%, aprotinin to 0.3 TIU (trypsin inhibitor units)/ml, benzamidine to 10 μM, leupeptin to 10 μg/ml, soybean trypsin inhibitor to 100 μg/ml and PMSF to 2 μM. Some lysates also were prepared in the presence of 50 mM β-glycerophosphate, 50 mM NaF and 100 μM $NaVO_4$ to block phosphatase activity, but phosphorylation extent was not influenced by their inclusion. Cell suspensions were disrupted by pipetting, then centrifuged for 1–2 min in a microcentrifuge. The supernatant was recovered and either directly applied to the Sepharose CL-6B column (28 cm × 1 cm) at 4 °C in the m^7GTP-Sepharose buffer, or stored at −80 °C until use. Samples of ~ 1 ml were collected at approx. 0.3 ml/min with a peristaltic pump. Aliquots (700 μl) were removed from each fraction, precipitated with 2 vol. of 100% ethanol overnight at −20 °C, collected by microcentrifugation for 30 min at 4 °C, resuspended in 50 μl of 1 × SDS sample buffer, heated for 2 min at 98 °C, and analysed by one-dimensional SDS gel electrophoresis (1DGE) and immunoblotting. The Amido Schwartz staining pattern of the blot showed the predicted correlation between elution volume and protein molecular mass. The principal exception was that in the excluded material a range of protein sizes, including some quite small species, were detected.

[^{35}S]Methionine protein labelling

One well of a 24-well tissue culture plate was used per time point for protein synthesis rate determinations. Cells were treated or mock-treated at time zero. Aliquots of DMEM (500 μl) containing 2 μCi/ml [^{35}S]methionine were added to wells for 30 min. Reactions were terminated and the contents of wells harvested at 40, 50 and 60 min by the addition of 2 ml of 4 °C EBSS/10 μg/ml cycloheximide. Therefore, the incorporations represent labelling amount in a 10, 20 or 30 min interval, corresponding to 30–40, 30–50 and 30–60 min relative to initiation of treatment. Cells were washed once on the plate, then lysed in 100 μl of GLB or

LSB (low salt buffer) [25 mM Hepes (pH 7.2), 65 mM KCl, 0.5 mM $MgCl_2$, 0.5 % Triton X-100, plus protease inhibitors, as detailed above] and 10 μl aliquots were counted by trichloroacetic precipitation and GF/C filter collection. Incorporation over the 30 min labelling interval was roughly linear and extrapolated to zero at label addition time in all cases.

Polysome analysis

Cells were washed as described above. The cell pellets were lysed in 4 °C polysome buffer [125 mM KCl, 37.5 mM $MgCl_2$, 25 mM EGTA, 10 mM Hepes (pH 6.8), 1 mM dithiothreitol, 10 μg/ml cycloheximide] by homogenization, nuclei and debris were removed by centrifugation for 30 s in a microfuge, and the supernatants were layered on 20–45 % sucrose gradients (w/v) made in polysome buffer. Gradients were centrifuged at 220000 ***g*** for 2 h at 4 °C in an SW41 rotor. Gradients were scanned in an ISCO scanning gradient fractionator at 254 nm using upward displacement with 50 % sucrose.

[^{3}H]Thymidine labelling

SMCs were seeded into a 24-well plate at low density. Upon reaching 80 % confluence, cells were cultured in 0.5 % serum for 48 h. For treatments, one well of a 24-well tissue culture plate was used per time point. Cells were treated or mock-treated at time zero with 0.5 μCi/ml [^{3}H]thymidine. All wells were harvested/stopped 24 h later by the addition of 2 ml of 4 °C EBSS. Cells were washed once on the plate, then lysed in 100 μl of GLB, as described above, and duplicate 50 μl samples were counted by TCA precipitation and GF/C filter collection (Whatman, Maidstone, Kent, U.K.).

[^{32}P]inorganic phosphate labelling

Cells were seeded into a 6-well plate, and used at 75–95 % confluence. Labelling media was DMEM lacking phosphate (ICN) supplemented with 1 mCi/ml [^{32}P]inorganic phosphate. Cells were treated or mock-treated at time zero. At 15 min intervals, the growth medium was removed and replaced with 500 μl of labelling medium for 15 min. Lysates (250 μl) were prepared in m^{7}GTP-Sepharose buffer as described above. Aliquots of 10 μl were removed, and the remainder incubated with 50 μl of a 50 % slurry of m^{7}GTP-Sepharose (Amersham Pharmacia) for 15–60 min (in different replicates) at 4 °C with manual shaking every 2–5 min. The Sepharose was collected by microcentrifugation for 30 s, and a 12.5 μl sample was removed from the supernatant. The Sepharose was washed once with 500 μl of m^{7}GTP-Sepharose buffer by microcentrifugation. The pellet was incubated with 2 × SDS-sample buffer for 2 min at 98 °C, vortexed vigorously, microcentrifuged for 30 s, and the supernatant removed and analysed, along with input and non-bound aliquots, by 1DGE (Laemmli system) and immunoblotting. The blot was exposed to film 1–8 days (depending on the experiment) before incubation with anti-eIF4E antisera. The autoradiogram quantified the incorporation in affinity-purified eIF4E (and verified that overall ^{32}P-labelling was not affected by the oxidant treatments) and the immunoblot verified that (i) all detectable eIF4E was selected by the m^{7}GTP-Sepharose incubation, and (ii) equivalent amounts of eIF4E were recovered from all treatment wells such that the autoradiogram band intensity represented molar incorporation rate.

RESULTS

The vascular cells involved in atherogenesis include endothelial cells, vascular SMCs, and macrophages. OxLDL and model oxidants can increase cell proliferation in responsive cell types (e.g. vascular SMCs [36]) and others [37]). This was confirmed in the present study (Figure 1A): HPLC-purified oxLDL, but not total LDL (tLDL) (containing $\leqslant 2$ % oxLDL), increased [^{3}H]-thymidine incorporation in SMCs. The oxLDL used in these studies was purified from naturally occurring, total LDL by HPLC as a minor, more electro-negative, fraction [33], rather than by metal-induced or other *in vitro* forms of oxidation.

To investigate whether oxidative stress could cause a rapid direct activation of the general translational machinery, the protein synthesis rate before and following oxidative stress was determined by pulse-labelling and polysome profile analysis in exponential-growth-phase cells. A small to modest increase in translation rate was observed during the first hour of treatment of cells with the model oxidants H_2O_2 and DMNQ (approx. 1.9- and 1.3-fold respectively) by [^{35}S]methionine pulse-labelling (Figure 1C). OxLDL increased amino acid incorporation by approx. 10 % (not statistically significant). Increased ribosomes in the active polysomal fraction were detected in the H_2O_2-treated cells (Figure 1B). No distinguishable increase was observed following DMNQ treatment (results not shown), presumably because the extent of increase (1.3-fold) is too small to quantitatively detect by this technique.

The proliferation assays were carried out with SMCs, since these are the principal vascular cell types that respond to oxidative stress by increased proliferation. However, our SMC cultures proved extremely sensitive to cell culture manipulations, such that significant activation of metabolic events [e.g. extracellular signal-related kinase (ERK) activity and the eIF4E phosphorylation response (see below)] frequently has been observed following only a media change (no agonist). For this reason, for the protein synthesis measurements described above (and following), other vascular cell types were principally used, since it proved difficult to quantitatively distinguish specific oxidative stress-induced events from manipulation-induced events when the activated signal is only 1.3–2-fold the basal amount, as is the case for protein synthesis rate in untreated versus treated cells.

OxLDL and LOOH cause eIF4E phosphorylation in vascular cells

Vascular cells treated with oxLDL activate the transcription of many cytokine and growth factor mRNAs [1], several of which are predicted to be translated relatively poorly based on their 5′UTR structure, as described in the Introduction section. Increased eIF4E activity could specifically increase the translation rate of these mRNAs. Furthermore, eIF4E activity is known to be rate-limiting for general translation, and its activation could contribute to, or cause, the oxidant-induced increased translational rate documented above (Figures 1B and 1C).

To determine whether eIF4E was rapidly activated by oxLDL treatment in vascular cells, cells were treated with naturally-oxidized LDL in LDL-deficient serum, and the phosphorylation state of eIF4E was quantified as a measure of its activity; additional activity assays are described in subsequent sections. The phosphorylation state was determined by displaying unlabelled cell lysates by two-dimensional IEF/SDS/PAGE, electrophoretic transfer to PVDF membrane, and identification of eIF4E by reaction with anti-eIF4E antisera and ECL® detection. Immunoblot panels representing a portion of the entire gel were used (see Figures 2B and 2C). Quantitation was by densitometry of ECL® films exposed for varied intervals to ensure linearity.

In the first series of experiments, endothelial cells were treated with oxLDL or tLDL. Prior to treatment, approx. 10–20 % of

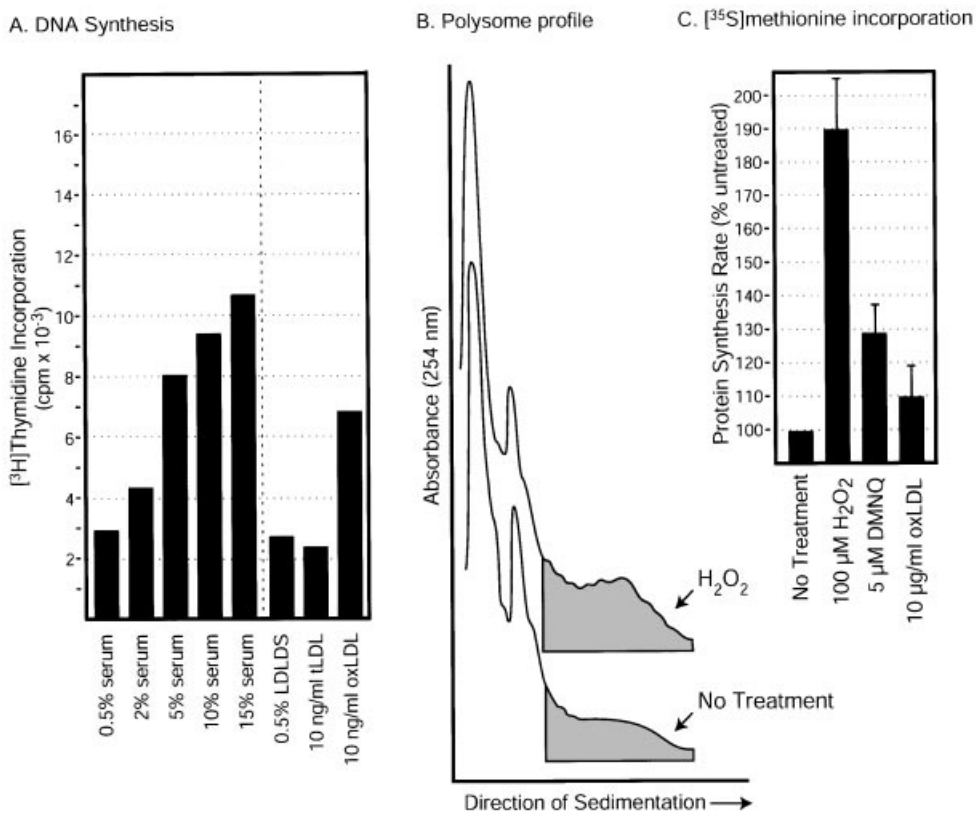

Figure 1 Activation of protein and DNA synthesis by oxidative stress

(**A**) Rabbit SMCs, at approx. 80% confluency, were transferred to 0.5% serum for 24–48 h. Medium was replenished with fresh DMEM containing various amounts of serum, or DMEM containing 0.5% LDL-deficient serum (LDLDS) without, or supplemented with, total or oxLDL, and 0.5 μCi/ml [^{3}H]thymidine. After 24 h the amount of incorporated thymidine was determined as described in the Experimental section. Different concentrations of LDLs were evaluated (results not shown); the data represent the maximal differential response to oxLDL. (**B**) J774 macrophage cells at, or near, saturation density were treated with 100 μM H_2O_2 in PBS for 15 min, returned to standard growth medium for 45 min, then lysed and analysed by sucrose density centrifugation for polysome content, which was assessed by continuous scanning at 254 nm. Profiles for untreated (control) and H_2O_2-treated cells are shown. (**C**) J774 macrophage cells were treated with 100 μM H_2O_2 in PBS, or only PBS, for 15 min, returned to standard growth medium for 15 min, then transferred into labelling medium (Cys-, Met-free DMEM containing 10% FCS and 2 μCi/ml [^{35}S]methionine). Cells were lysed and trichloroacetic acid-precipitable [^{35}S]methionine incorporation was determined at 10, 20 and 30 min of incubation. Protein synthesis rate is reported as the slope of the incorporation line, relative to the untreated (PBS) sample. DMNQ was added directly to the cell growth medium, and oxLDL treatment (and mock treatment) was in 0.5% LDLDS, as in (**A**) above. Values reported represent the mean for 2–4 experiments.

the eIF4E was in the phosphorylated state (Figure 2A, panel C), based on densitometric scanning. In separate experiments, this pre-treatment value has ranged from 10–35% (see other panels, and later Figures), which is characteristic of the range observed in other cell types. Following treatment with 10–20 μg/ml oxLDL, there is a progressive, time-dependent increase in the fraction of phosphorylated eIF4E that plateaus at around 60–70% after approx. 2 h (Figure 2C). This final level of phosphorylation is similar to that observed in other studies using potent inducers of eIF4E phosphorylation such as PMA (e.g. [38]; and R. Duncan, unpublished results). This extent was not attained in every experiment: the maximum phosphorylation level in an experiment typically ranged from approx. 45 (e.g. Figure 2D) to approx. 70% (note that even the lower range represents a two-fold increase). The hyperphosphorylation response to oxLDL is dose-dependent: 10 μg/ml is required to optimally induce phosphorylation (Figure 2D) and 20 μg/ml produces a quantitatively similar response (results not shown). Higher amounts were not investigated; treatment with 10–20 μg/ml oxLDL causes minimal ($< 20\%$) cytotoxicity, but as the amount is increased above 20 μg/ml significant cytotoxic effects begin to be observed with these cells (results not shown). Treatment of cells with tLDL did not cause increased eIF4E phosphorylation (results not shown).

A component of oxLDL that may contribute to oxidative stress is LOOH. To investigate whether LOOH treatment could cause increased eIF4E phosphorylation, endothelial cells were treated with 10 μM LOOH for various lengths of time. Paralleling the results with oxLDL, a time-dependent increase in eIF4E phosphorylation, reaching a plateau at 60–70% phosphorylation, was observed (Figure 2B). In other experiments carried out for longer treatment intervals, no further increase in phosphorylation state was observed. As discussed above for oxLDL, 10 μM LOOH approaches the cytotoxic threshold.

To determine whether the response to oxLDL and LOOH is common to vascular cell types, endothelial cells, macrophages and SMCs were treated with 20 μg/ml oxLDL or 10 μM LOOH for 2–3 h, and the extent of eIF4E phosphorylation was quantified. Significantly increased phosphorylation was measured in every case (Figure 2A). The lower amount of phosphorylation observed in oxLDL-treated macrophages, that was not statistically significant, may indicate a relatively lower sensitivity that reflects their scavenger/detoxifying role. The more pronounced response of SMCs was characteristic of this

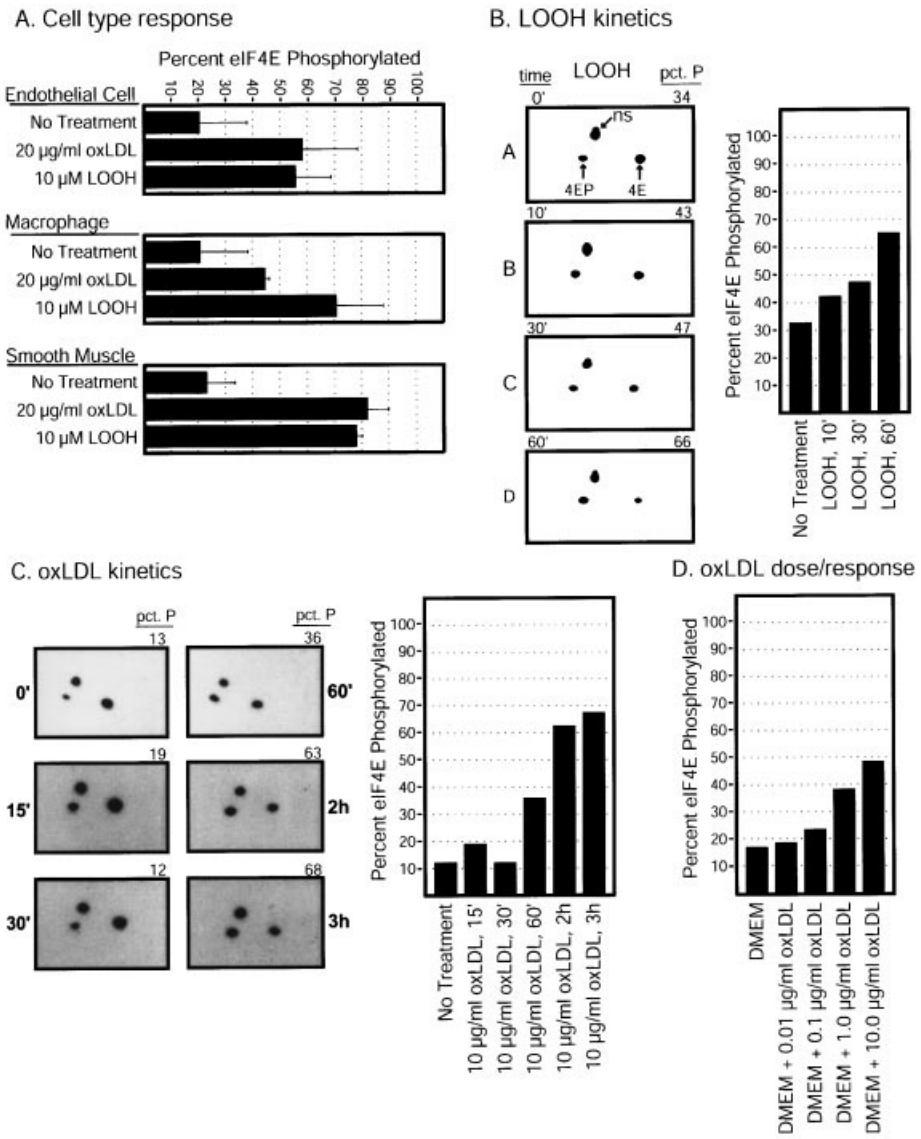

Figure 2 eIF4E phosphorylation by oxLDL and LOOH in vascular cells

Vascular cells were propagated and treated as described in the Experimental section. Following treatment, the extent of eIF4E phosphorylation was determined by two-dimensional IEF/SDS/PAGE and immunoblotting, as described in the Experimental section. (**A**) Treatments with oxLDL (120 min) and LOOH (60 min) in three vascular cell types. Values represent the mean for 2–10 determinations. (**B**) Kinetics of eIF4E phosphorylation by LOOH in endothelial cells, including representative immunoblot sectors used to quantify eIF4E phosphorylation. The locations of the two eIF4E spots (unphosphorylated and phosphorylated) are indicated, along with the location of an additional non-eIF4E cross-reactive spot (ns). Blots were scanned densitometrically, and the quantified results are depicted to the right. (**C**) Kinetics of eIF4E phosphorylation by oxLDL in endothelial cells; sectors and analysis as in (**B**). (**D**) Dose/response of eIF4E phosphorylation by oxLDL in endothelial cells. Results in (**B**, **C** and **D**) depict representative experiments of analyses repeated 2–3 times. pct. P, percent eIF4E phosphorylated.

cell type, and observed with numerous other oxidant stress-inducing agents.

Compounds that increase intracellular reactive oxgen species (ROS) cause eIF4E phosphorylation in vascular cells

The preceding results suggested that increased eIF4E phosphorylation might be a general response to oxidative stress, with significance beyond oxLDL and its oxidized components and their interactions with vascular cells. To determine whether model compounds that induce oxidative stress promoted increased eIF4E phosphorylation, vascular cells were treated with the oxidants H_2O_2 (as a bolus source of oxidant), glucose/glucose oxidase (which continuously propagates H_2O_2), and the quinones menadione and DMNQ. Menadione acts as an oxidant by reacting with and depleting GSH and by conjugating with proteins and other reactive cellular macromolecules. Oxidant stress caused by DMNQ allows the specific determination of the relative contribution of these two components, because it cannot conjugate due to its reactive conjugating sites being blocked by two methyl groups.

All oxidizing compounds tested induce a high level of eIF4E phosphorylation, typically in the range of 70–90%, in all the vascular cell types (Figure 3A). The induction is dose-dependent

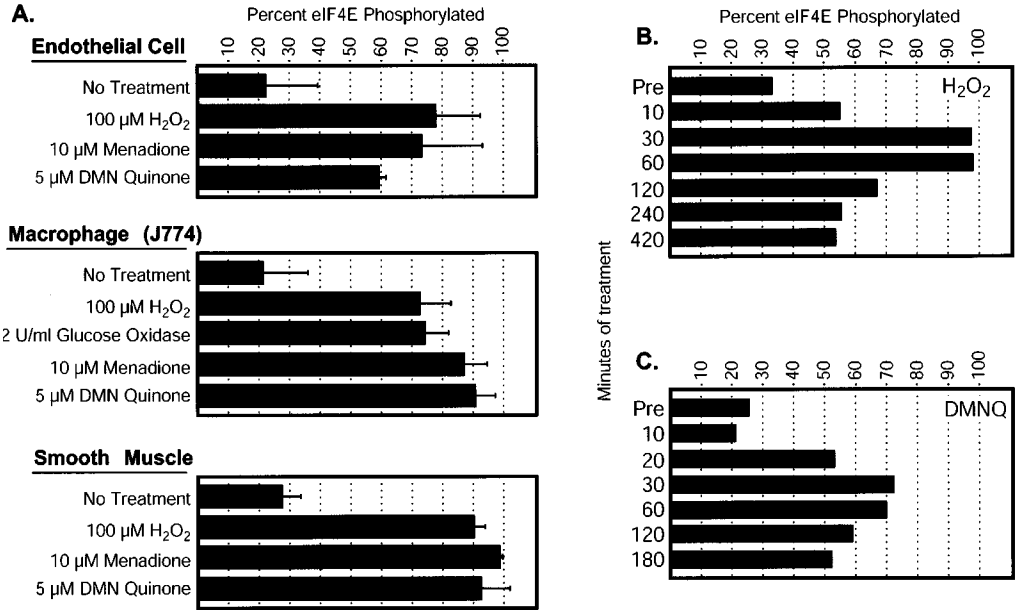

Figure 3 eIF4E phosphorylation by oxidants in vascular cells

Analyses were carried out as described in Figure 2 legend, and Methods. (**A**) Treatments with H_2O_2, DMNQ, menadione, and glucose/glucose oxidase (glucose was provided at 5 mM) in three vascular cell types. Values represent the mean for 2–10 determinations. (**B**, **C**) Kinetics of eIF4E phosphorylation by H_2O_2 (**B**) and DMNQ (**C**) in J774 cells. Results in (**B**) and (**C**) depict representative experiments of analyses repeated 2–3 times. U, units; Pre, pre-treatment.

(results not shown). Maximal phosphorylation occurs at the concentrations reported in the Figure. Kinetic examination of the response indicates that it occurs rapidly following oxidant treatment; examples with two oxidant agonists are shown (Figure 3B, H_2O_2; Figure 3C, DMNQ). The response to bolus H_2O_2 treatment is maximal within 30 min, persistent to 60 min, and then decreases up to 7 h; after 2 h $> 60\%$ of eIF4E remains phosphorylated, and at 4 and 7 h the extent of phosphorylation remains significantly elevated relative to before treatment (Figure 3B). The kinetic response to DMNQ is similar: in the example shown, the extent of maximum phosphorylation is lower (Figure 3C), but in several other replicates, DMNQ proved at least as potent an inducer. The induction by DMNQ clearly demonstrates that conjugation is not required for eIF4E phosphorylation induction, and implicates reduced GSH levels, or events induced by GSH depletion, in the response.

Oxidants increase eIF4E phosphorylation rate and association with eIF4G

When eIF4E associates with eIF4G/4A to form the eIF4F complex, there is a substantial increase in its activity in several partial reactions characterizing the initiation phase of translation [29]. It has also been suggested that eIF4E activity is better quantified by the rate of phosphate labelling, which includes phosphate turnover rate as a component, rather than by absolute extent of phosphorylation [39], based on the hypothesis that phosphate turnover comprises an aspect of recycling/re-utilization.

The ability of oxidative stress to increase both eIF4E association with eIF4G and the eIF4E phosphate labelling rate were determined, to provide additional evidence that oxidative stress activates eIF4E-dependent translation. First, lysates from untreated and H_2O_2-treated endothelial cells were passed over a size-exclusion Sepharose CL-6B column. eIF4E, a relatively small protein (approx. 25 kDa), elutes relatively late in fractions 16–20 [see Figure 4A, showing endogenous eIF4E; verified by chromatography of purified eIF4E (results not shown)]. When contained in multi-protein complexes of high molecular mass, eIF4E is eluted significantly faster, in the excluded volume fractions 9–10. In untreated endothelial cells, virtually all the immunologically detectable eIF4E elutes in the low-molecular-mass, monomeric, included region (Figure 4A, top panel). In H_2O_2-treated endothelial cells, the amount of low-molecular-mass eIF4E is significantly reduced, correlating with an increase in high-molecular-mass eIF4E (Figure 4A, bottom panel). The latter presumably represents eIF4F complexes, perhaps also complexed with other translational components. The results are strongly suggestive of increased eIF4E activity caused by oxidant treatment.

Second, cells were pulse-labelled with 1 mCi/ml [^{32}P]phosphate for 15 min at intervals after H_2O_2 treatment, and eIF4E and associated proteins were purified by batch-wise affinity chromatography using m^{7}GTP-Sepharose. A significant but not dramatic increase in eIF4E labelling was detected in H_2O_2-treated cells (Figure 4B), which ranged from approx. 1.5–2.5-fold in four replicate experiments. The labelling rate appeared to return to control levels with increasing time after treatment. This enhanced labelling rate is entirely consistent with the mass distribution shift detailed in Figure 3, suggesting that the fraction of phosphorylated eIF4E could approximately double every 15 min. However, it does not indicate that eIF4E phosphate turnover rate is enhanced to a greater extent than the change in phosphorylation distribution.

The phosphorylation state of other initiation factor proteins is not affected by oxidant treatment

eIF4E activity is also influenced by the binding of the inhibitory protein eIF4E-BP1 to the eIF4G interaction site on eIF4E

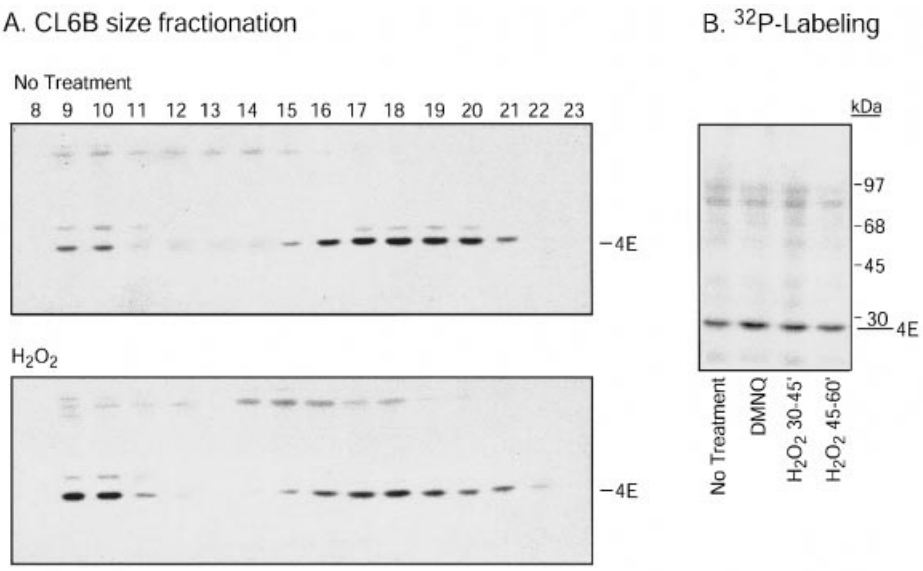

Figure 4 Activity of eIF4E assessed by its associations with other proteins in large complexes, determined by CL-6B column chromatography, and [^{32}P]phosphate labelling

(**A**) J774 cells were incubated in PBS, or PBS containing 100 μM H_2O_2, for 15 min, then returned to standard growth medium for 45 min. Lysates were prepared in m^{7}GTP–Sepharose analysis buffer and analysed as described in the Experimental section. (**A**) One-dimensional SDS/PAGE immunoblot analysis of eIF4E. Upper panel, mock (PBS-treated) and lower panel, H_2O_2-treated. Fraction numbers are indicated at the top of the blot. Faint non-eIF4E bands were also detected. The location of eIF4E was determined by co-electrophoresis of purified eIF4E (results not shown). Excluded material began to elute around fraction 9. Amido schwartz staining revealed a heterodisperse array of protein molecular masses in fractions 9 and 10. Between fractions 11–23 there was a progressive decrease in average protein size. (**B**) J774 cells were incubated in PBS, or PBS containing 100 μM H_2O_2, for 15 min, then returned to standard growth medium. At intervals, cells were labelled for 15 min with [^{32}P]phosphate and processed for autoradiography as described in the Experimental section. 5 μM DMNQ-treated cells were labelled 60–75 min into the treatment. Proteins transferred to PVDF were exposed for autoradiography, and subsequently the PVDF was probed with anti-eIF4E, which verified that approx. equal amounts of total eIF4E were present in each lane. Results depict representative experiments of analyses repeated 2–3 times.

[27,40]. eIF4E-BP1 binds strongly to eIF4E in its dephosphorylated state; phosphorylation decreases the affinity, freeing eIF4E to interact with eIF4G forming active high-molecular-mass complexes. The phosphorylation status of eIF4E-BP1 was determined in macrophages by immunodetection of two- (or one-) dimensional gel-resolved unlabelled proteins. A diverse, complex array of isoforms, most of which are derived from the gene encoding eIF4E-BP1 [41], are detected (Figure 5A). An interpretative diagram indicating the most prominent detected spots, based on many such 2DGE analyses (where 2DGE is two-dimensional gel electrophoresis using IEF in the first dimension and 1DGE in the second dimension), is shown in Figure 5(A) (top right panel). The depicted isoform distribution is specific to macrophages; very different isoform distribution patterns are detected in other cell types ([41]; R. F. Duncan, unpublished work). Treatment with oxidants does not produce any marked changes in the relative distribution pattern (that is, of the fractional percentage of eIF4E-BP1 in each spot quantified). The significance, if any, of the small redistributions and spot location changes cannot be currently assessed. For comparison, the effect of treating cells with anisomycin is shown (lower centre panel of Figure 5A). In this case, there is decreased representation of spots 1 and 4–7, and enhanced representation in the most acidic spots 8–11; these are predicted to be the most phosphorylated isoforms (located to the left in this panel). Though their identity as phosphoproteins was not explicitly verified in this study, studies by ourselves and Sonenberg and co-workers have confirmed that these are phosphorylated isoforms and that each more acidic migrating spot reflects phosphorylation at an additional phosphorylation site [42]. Anisomycin in these cells is a potent inducer of eIF4E-BP1 phosphorylation (R. Duncan, unpublished results) providing a useful positive control for an enhanced phosphorylation response. Cell lysates were also examined by 1DGE/immunoblotting. In all cell lysates, three eIF4E-BP1 bands were detected. There was no marked redistribution following treatment with any inducer of oxidative stress (Figure 5A, lower right panel); a modest shift of β into γ forms (more slowly migrating, higher apparent molecular mass) induced by oxidants may occur. Concurrent treatment with rapamycin or wortmannin caused the predicted shift into faster migrating (α) forms, paralleling results of others using these signal transduction modulators, and confirming that signal transduction pathways capable of modulating eIF4E-BP1 phosphorylation are operative in these cells. As detailed elsewhere [41], the 2DGE resolution of eIF4E-BP1 reveals a striking complexity of isoforms, whereas the 1DGE analysis, while simple to interpret, can obscure numerous potentially significant alterations in eIF4E-BP1 isoform distribution.

The phosphorylation state of other initiation factor proteins is correlated with translation machinery activity [43]. To determine if the phosphorylation state of other initiation factor proteins was affected by oxidative stress, lysates were prepared, proteins resolved by IEF/SDS/PAGE, and eIF proteins detected by their corresponding antibodies. As noted above, IEF displacements reflect changes in the mass of factor protein in the phosphorylated state. eIF4B phosphorylation is frequently enhanced in concert with eIF4E following stimulation by many agonists that increase the rate of protein synthesis [22,43]. However, eIF4B phosphorylation is not increased in response to oxidative stress due to H_2O_2 treatment (Figure 5B). This suggests that the signalling

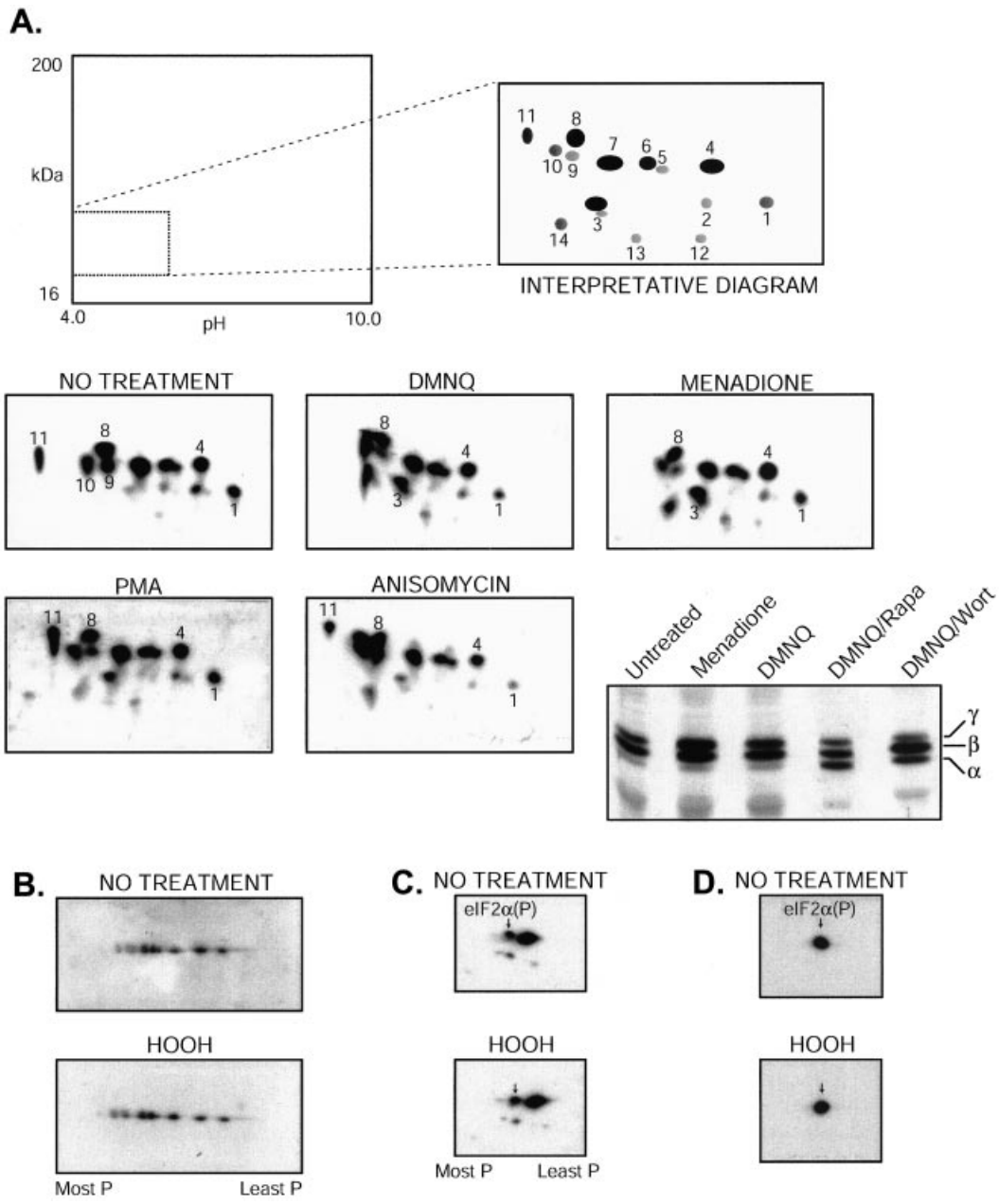

Figure 5 Oxidative stress effects on eIF4E-BP1

(**A**) Control and oxidant-treated J774 cells were lysed in GLB extraction buffer as described in the Experimental section, and analysed by two-dimensional IEF/SDS/PAGE and immunoblotting using anti-rat eIF4E-BP1 (PHAS-I) antisera. Approx. equal amounts of protein were loaded on to each first-dimension gel. Sections of the complete blot are shown in each of the lower 5 panels. The left border of each panel is the most acidic boundary of the sector. The upper left schematic depicts the portion of the entire gel excised for analysis of the eIF4E-BP1 sector. The upper right schematic identifies the most commonly detected prominent spots (some of which are also identified in the other panels). Patterns obtained pre-treatment and following treatment with 5 μM DMNQ, 10 μM menadione, 100 nM PMA and 33 ng/ml anisomycin for 1 h are depicted. Since the most acidic eIF4E-BP1 isoforms run at the very acidic edge of the isoelectric focusing gradient, they occasionally become compressed and curved ('smiling') during second dimension analysis, as is seen in this Figure in the DMNQ and anisomycin panels. Analysis of H_2O_2 is not depicted due to recurrent technical difficulties. eIF4E-BP1 was also analysed by 1DGE/immunoblotting on 12.5% PAGE. Results are depicted in the lower right panel, and treatments were as detailed above, and are listed at the top of the panel. Rapamycin (Rapa) treatment was at 20 ng/ml and wortmannin (Wort) at 100 nM, both added 30 min prior to oxidant treatment and retained during the treatment interval (60 min). (**B**–**D**) J774 cells were treated with H_2O_2, as described above, for 1 h and lysates prepared in AMLYS, resolved by 2DGE, transferred to PVDF membrane and probed with antisera to eIF4B (**B**), antisera to eIF2α (**C**), or antibodies that only recognize the S51 phosphorylated isoform of eIF2α (**D**).

pathways activated by oxidative stress are relatively restricted, leading to enhanced eIF4E phosphorylation but not other frequently correlated protein phosphorylations (i.e. eIF4E-BP1 and eIF4B). eIF2α phosphorylation has been observed as a frequent correlate of cellular stress [43]. eIF2α phosphorylation causes an inhibition of its activity, and by extension, of overall protein synthesis rate. Since mild oxidative stress, as investigated in this report, activates rather than inhibits protein synthesis, we would not expect it to cause increased eIF2α phosphorylation. Nonetheless, to verify this prediction, eIF2α

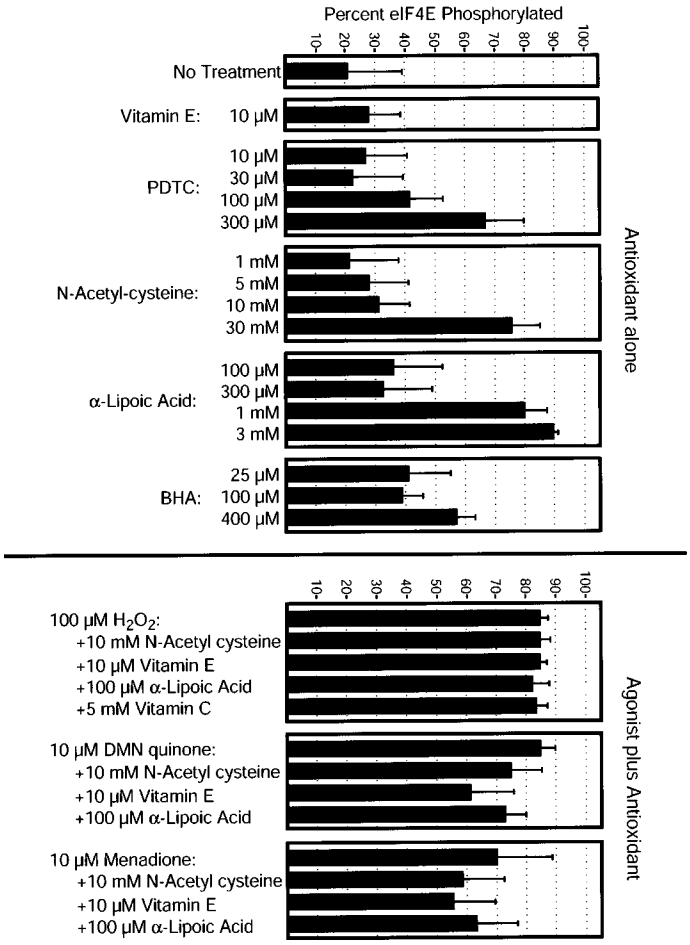

Figure 6 Effects of anti-oxidants on oxidant-induced increased eIF4E phosphorylation

Upper panel: J774 cells were pre-treated with the types and amounts of anti-oxidants indicated for 2 h [PDTC, BHA, vitamin C (not shown), and NAC] or overnight (approx. 16 h) (vitamin E and lipoic acid). After pre-treatment, cells were lysed and processed for eIF4E phosphorylation quantification. Values reported represent the mean for 2–4 experiments. Lower panel: following anti-oxidant pre-treatment, J774 cells were treated with oxidants as indicated for 1 h, at which time lysates were prepared and analysed. Values reported represent the mean for 2–4 experiments. DMNQ concentration was modestly increased, based on apparent declining effectiveness of stock solution.

phosphorylation was investigated. No increase in its phosphorylation (Figures 5C and 5D, showing all eIF2α isoforms and only phosphorylated eIF2α by using phospho-specific antibodies respectively), confirming predicted results. The J774 cells have reproducibly shown relatively high levels of eIF2α phosphorylation in their exponential growth phase, which may be correlated with the relatively modest fraction of ribosomes in polysomes (Figure 1).

Antioxidants also can increase eIF4E phosphorylation in vascular cells

To provide confirmation that increased intracellular ROS could increase eIF4E phosphorylation, the effects of pre-treating vascular cells with several anti-oxidant compounds were investigated. Initially, the effects of just the anti-oxidant pre-treatment on eIF4E phosphorylation were determined. At relatively high anti-oxidant concentrations used in studies by others demonstrating anti-oxidant suppression of an oxidant stress-based response, all the anti-oxidants tested increased eIF4E phosphorylation (Figure 6, upper panel), with the exception of vitamin E. These agonistic anti-oxidants included 300 μM 1-pyrrolidine-carbodithioic acid (PDTC), 30 mM *N*-acetylcysteine (NAC), 1 mM α-lipoic acid (ALA), and 400 μM BHA. Further consideration of this apparently paradoxical response is presented in the Discussion section. The agonistic action of these anti-oxidants at concentrations commonly employed to block an oxidant-induced response precluded investigation of their ability to suppress eIF4E phosphorylation by oxidants. The ability of the lower concentrations, which caused lower increases in eIF4E phosphorylation, to suppress oxidant-induced phosphorylation was investigated.

NAC, vitamin E, vitamin C, both vitamin E and C combined, and ALA did not significantly suppress oxidant-induced eIF4E phosphorylation by H_2O_2, DMNQ, or menadione (Figure 6, lower panel, and results not shown). A small measure of suppression by vitamin E may occur, but the extent varied significantly from virtually none to approx. 50 %, and the extent depicted is not statistically significant. Catalase or glutathione peroxidase/GSH added to the treatment media were effective at suppressing H_2O_2-induced eIF4E phosphorylation as predicted (results not shown); they had no effect on quinone-induced phosphorylation. To verify that anti-oxidant treatments ineffective at blocking eIF4E phosphorylation were largely suppressing intracellular ROS production, ROS levels following 100 μM H_2O_2 treatment were measured by 2′,7′-dichlorofluorescein (DCF) fluorescence, without and with anti-oxidant pre-treatment. A combination of 10 μM vitamin E and 100 μM vitamin C suppressed the intracellular accumulation of ROS induced by H_2O_2 by $>95\,\%$, as predicted, based on DCF fluorescence measurements (results not shown); this combination caused no detectable inhibition of the induction of eIF4E phosphorylation, suggesting that an oxidant-sensitive membrane-proximal signalling cascade initiates an intracellular pathway that is not dependent on subsequent intracellular ROS generation.

DISCUSSION

Oxidative stress is considered to be a likely initiator of atherosclerotic events, causing the increased synthesis of numerous mitogenic factors that contribute to the hyperproliferation of SMCs and vascular plaque formation [5]. We have noted that many of the mRNAs encoding these pro-mitogenic factors contain 5′UTR secondary structure-burdened mRNAs, which impede their translation. We hypothesized that increased eIF4E activity would be a component of the atherogenic response, promoting the translation of these mRNAs in vascular cells exposed to oxidative stress. A function for eIF4E and translation regulation in the early atherogenic response would constitute a significant new locus of pathophysiology.

Oxidative stress proves to be a potent inducer of eIF4E phosphorylation in all types of vascular cells. The response is induced rapidly by relatively low, non-cytotoxic, exposures to oxidants, including physiologically relevant forms such as oxLDL and oxidized lipid components, as well as model oxidants such as H_2O_2. Transient activation of eIF4E by oxidants may play a regulatory role in transiently boosting expression of potent growth-promoting proteins, for example in response to infection or wounding, whereas chronic oxidative stress is likely to have pathophysiological consequences at the level of translation by facilitating continued, inappropriate, over-expression of these proliferation-promoting proteins. Although eIF4E phosphoryl-

ation has traditionally been considered a modification that enhances translation [13], and we propose that it affects vascular physiology via this mechanism, recent reports have suggested that eIF4E phosphorylation has little effect on eIF4E function [44], and even inhibits overall translation [45]. However, Lachance et al. [31] observe that a non-phosphorylatable eIF4E isoform fails to support normal *Drosophila* development, indicating that phosphorylation is required for some aspect of eIF4E function. Oxidants that significantly enhance eIF4E phosphorylation do not inhibit global translation rate (and may modestly enhance it), but this could result from other pathways being targeted which override any inhibitory effects of eIF4E phosphorylation. Our brief screen of several other possible translation factor targets did not identify any other phosphorylation changes, though several possible targets [e.g. eIF4G and ribosomal protein S6 (rpS6)] were not analysed. An attractive hypothesis is that eIF4E phosphorylation primarily redirects translation to recognize a sub-category of mRNAs.

Identification of the mRNA targets translationally activated by oxidative stress is crucial to further progress. We have used 2DGE analysis of proteins to identify several whose synthesis is rapidly induced by oxidative stress (R. F. Duncan, unpublished work), though the total number of significantly affected proteins is relatively small (< 10). Identification of these candidates is in progress. Additional analyses focused directly on the mRNAs recruited in polysomes by oxidative stress may facilitate detection of more rare mRNAs whose protein products are below the level of detection of 2DGE analysis.

Numerous pathophysiological conditions have been proposed to be enhanced or precipitated by oxidative stress, including cancer, skin damage, diabetes and arthritis (e.g. [3,46]). A frequent corollary of these disease states is the overexpression of 5′UTR-burdened, cell-growth-promoting mRNAs, which is a hallmark of cancer, for example. Our results suggest that any situation involving chronic oxidative stress will promote protein synthesis from certain of these mRNAs, and as such constitute a significant component of the pathologic response. In addition, recent studies have suggested that low levels of oxidative stress accompany, and in some instances are required for, mitogenic responses elicited by peptide growth factors [epidermal growth factor ('EGF'), PDGF], cytokines, tumour promoter agents (PMA), and oncogenic proteins (e.g. *ras*) (reviewed in [47]). The eIF4E hyperphosphorylation response may thus constitute a component of a physiological proliferative metabolic response based in oxidative stress signalling, required for optimal expression of growth promoting proteins.

Several compounds previously documented to be potent inducers of eIF4E phosphorylation, including PMA, PDGF, and TNF-α [22], have subsequently been shown to activate some of their responses by ROS-dependent, oxidative stress-based pathways [47]. This conclusion has been based, in part, on demonstrating response suppression by anti-oxidants, such as 30 mM NAC. We were interested in determining if the eIF4E phosphorylation response to these agents required activation of an ROS-based signalling pathway. However, as presented in the Results section, we were unable to test high potently suppressing concentrations of anti-oxidants, because the compounds by themselves increased eIF4E phosphorylation. At lower levels which fail to significantly increase eIF4E phosphorylation, neither NAC, vitamin E, vitamin C, nor combined vitamins E and C, nor ALA could suppress phosphorylation caused by PMA or TNF-α treatments.

The 'activation' of eIF4E phosphorylation by anti-oxidants, as well as oxidants, has precedent in the activation of nuclear factor κB (NF-κB) [48]. Treatment of T- and B-cells with peroxides, paraquat, and menadione (as examples of oxidants), and PDTC and NAC (as examples of anti-oxidants), both efficiently increase NF-κB DNA binding and transactivation. The observation is complicated by the fact that certain anti-oxidants, such as PDTC, may activate because they perturb metal metabolism, and others, such as vitamin E, can act as pro-oxidants under certain circumstances. The activation of eIF4E by anti-oxidants parallels these observations. The specific basis for the anti-oxidant responsiveness remains unresolved at present.

Oxidants, such as H_2O_2, activate mitogen-activated protein (MAP)-family kinases, including ERK, p38, and c-Jun N-terminal kinase ('JNK') (e.g. [49]). Furthermore, recent characterization of the pathway leading to eIF4E phosphorylation suggests activation of either ERK1/2 or p38 promotes eIF4E phosphorylation via activation of MNK1 (MAP kinase signal-integrating kinase) [49–51]. In contrast with our results, Wang et al. [49] did not observe enhanced eIF4E phosphorylation following H_2O_2 treatment in 293 cells, even though MNK1 was strongly activated and phosphorylated eIF4E *in vitro*. This discrepancy may be analogous to other cell-type-specific discrepancies, where the phosphorylation of the substrates rpS6 [52,53] and eIF4E-BP1 [54] do not increase even though their regulatory kinases are activated in response to stress. In these instances, it has been suggested that the discrepant end-responses result from the relatively stronger activation of potent phosphatases which can reverse and suppress kinase-activation-induced target protein phosphorylation. Our studies with 293 cells using low doses of H_2O_2 (as reported in the present study) have been equivocal, with significant changes detected in some experiments, but no effects observed in others (R. F. Duncan, unpublished work). Our results suggest, at the least, that 293 cells are less sensitive to oxidative stress. We have observed that stresses, such as heat shock, which decrease or cause no increase in eIF4E and eIF4E-BP1 phosphorylation, apparently activate kinases specific for these factors [41]; this apparent contradiction is consistent with the disproportionate activation of highly potent phosphatases which mask the kinase activation. In the experiments of Wang et al. [49], hydrogen peroxide was used at 3 mM, which constitutes a severe stress for most cell types [including 293 cells, in our experience (R. F. Duncan, unpublished work)]; this could have contributed to the (proposed) disproportionate activation of phosphatases.

While this work was in progress, Rao [55] reported that H_2O_2 enhanced eIF4E phosphorylation in SMCs. Our findings are wholly in accord with this report in all major respects, and support the conclusion that oxidative stress, when occurring at non-cytotoxic, signalling levels, potently enhances eIF4E phosphorylation. Rao observed no effects on overall protein synthesis in SMCs; our experiments also could not detect an effect of H_2O_2 on overall translation in SMCs, though results were equivocal, as described in the Results section. Even in the macrophage cells, the stimulation was not observed in every experiment. Our studies have extended the range of eIF4E phosphorylation enhancement to several other vascular cell types, and we have also determined that it occurs in epithelial cells (R. F. Duncan, unpublished work). This suggests that the observed activation of eIF4E will probably influence the translation of 'burdened' mRNAs as a general correlate of mild oxidative stress, with attendant ramifications on cell pathophysiology whenever chronic oxidative stress occurs.

At this point we cannot resolve whether the change in translation rate is specifically a consequence of eIF4E phosphorylation, or partly or wholly based on other modifications of the translational machinery. In our studies of oxidative stress, we

have shown that neither eIF4E-BP nor eIF4B shows phosphorylation changes; however, oxidative stress also activates rpS6 kinase (pp70S6K) ([56]; R. F. Duncan, unpublished work) leading to increased rpS6 phosphorylation [56]. Other as yet uncharacterized translation alterations may occur as well. Ideally, to prove that the eIF4E phosphorylation was the cause of translational activations, cells would be treated with a reagent that uniquely increased eIF4E phosphorylation. In practice, oxidative stress appears to come closer to this goal than many other eIF4E phosphorylation inducers, since correlated changes in most other eIFs are not observed.

In conclusion, our results suggest that vascular cells respond to oxidative stress by activating eIF4E and hence affecting protein synthesis. The pathway probably involves the activation of ERK and/or p38 MAP-family protein kinases, which are both activated by oxidative stress in these cells (R. F. Duncan, unpublished work). In line with this suggestion, we have observed that MNK1 is activated, and that co-ordinate inhibition of both MAP-family protein kinases suppresses the oxidant stress-induced eIF4E phosphorylation (R. F. Duncan, unpublished work). Oxidative stress-based signalling pathways are emerging as a new class of physiological mediators, involved in responses, ranging from vascular constriction/relaxation to cell growth control [47]. When appropriately regulated, oxidative stress signalling mediates essential responses to environmental cues. However, chronic conditions of oxidative stress, such as those which occur during arthritis, excessive UV exposure, or dysregulated ras/rac activity, are likely to tilt the response towards pathogenesis. We suggest that inappropriate eIF4E activation constitutes one component of this pathogenic response.

We thank Dr J. C. Lawrence Jr. (Department of Pharmacology, University of Virginia Health System, Charlottesville, VA, U.S.A.) for providing the anti-PHAS-I antisera, and Drs A.-C. Gingras and N. Sonenberg (Department of Biochemistry and McGill Cancer Centre, McGill University, Canada) for antisera to eIF4E-BP1. We thank Dr Derrick Han (Department of Molecular Microbiology and Immunology, University of Southern California) for assistance in measuring ROS by DCF. This research was supported by NIH grant HL50350 (to A.S.) and a Wright Foundation award (to R.F.D.).

REFERENCES

1 Ross, R. (1993) The pathogenesis of atherosclerosis: a perspective for the 1990s. Nature (London) **362**, 801–809
2 Ross, R. (1999) Mechanisms of disease: atherosclerosis – an inflammatory disease. New Eng. J. Med. **340**, 115–126
3 Halliwell, B. (1993) The role of oxygen radicals in human disease, with particular reference to the vascular system. Haemostasis **23**, 118–126
4 Alexander, R. W. (1995) Hypertension and the pathogenesis of atherosclerosis. Oxidative stress and the mediation of arterial inflammatory response: a new perspective. Hypertension **25**, 155–161
5 Berliner, J. A. and Heinecke, J. W. (1996) The role of oxidized lipoproteins in atherogenesis. Free Rad. Biol. Med. **20**, 707–727
6 Rao, C. D., Pech, M., Robbins, K. C. and Aaronson, S. A. (1988) The 5′ untranslated sequence of the c-*sis*/platelet derived growth factor 2 transcript is a potent translational inhibitor. Mol. Cell. Biol. **8**, 284–292
7 Parkin, N. T., Darveau, A., Nicholson, R. and Sonenberg, N. (1988) *cis*-Acting translational effects of the 5′ noncoding region of c-*myc* mRNA. Mol. Cell. Biol. **8**, 2875–2883
8 Prats, A. C., Vagner, S., Prats, H. and Amalric, F. (1992) *cis*-acting elements involved in the alternative translation initiation process of human basic fibroblast growth factor. Mol. Cell. Biol. **12**, 4796–4805
9 Koromilas, A. E., Lazaris-Karatzas, A. and Sonenberg, N. (1992) mRNAs containing extensive secondary structure in their 5′ non-coding region translate efficiently in cell overexpressing initiation factor eIF4E. EMBO J. **11**, 4153–4158
10 Rosenwald, I. B., Lazaris-Karatzas, A., Sonenberg, N. and Schmidt, E. V. (1993) Elevated levels of cyclin D1 protein in response to increased expression of eukaryotic initiation factor 4E. Mol. Cell. Biol. **13**, 7358–7363
11 Shantz, L. M. and Pegg, A. E. (1994) Overproduction of ornithine decarboxylase caused by relief of translational repression is associated with neoplastic transformation. Cancer Res. **54**, 2313–2316
12 Kevil, C., Carter, P., Hu, B. and DeBenedetti, A. (1995) Translational enhancement of FGF-2 by eIF-4 factors, and alternate utilization of CUG and AUG codons for translation initiation. Oncogene **11**, 2339–2348
13 Gingras, A. C., Raught, B. and Sonenberg, N. (1999) eIF4 initiation factors: effectors of mRNA recruitment to ribosomes and regulators of translation. Ann. Rev. Biochem. **68**, 913–963
14 Sonenberg, N. (1988) Cap binding proteins of eukaryotic messenger RNA: functions in initiation and control of translation. Prog. Nucleic Acid Res. Mol. Biol. **35**, 173–207
15 Lazaris-Karatzas, A., Montine, K. S. and Sonenberg, N. (1990) Malignant transformation by a eukaryotic initiation factor subunit that binds to mRNA 5′ cap. Nature (London) **345**, 544–547
16 De Benedetti, A. and Rhoads, R. E. (1990) Overexpression of eukaryotic protein synthesis initiation factor 4E in HeLa cells results in aberrant growth and morphology. Proc. Natl. Acad. Sci. U.S.A. **87**, 8212–8216
17 Lazaris-Karatzas, A. and Sonenberg, N. (1992) The mRNA 5′ cap-binding protein, eIF-4E, cooperates with v-myc or E1A in the transformation of primary rodent fibroblasts. Mol. Cell. Biol. **12**, 1234–1238
18 De Benedetti, A., Joshi-Barve, S., Rinker-Schaeffer, C. and Rhoads, R. E. (1991) Expression of antisense RNA against initiation factor eIF4E mRNA in HeLa cells results in lengthened cell division times, diminished translation rates, and reduced levels of both eIF4E and the p220 component of eIF-4F. Mol. Cell. Biol. **11**, 5435–5445
19 Rinker-Schaeffer, C. W., Graff, J. R., De Benedetti, A., Zimmer, S. G. and Rhoads, R. E. (1993) Decreasing the level of translation initiation factor 4E with antisense RNA causes reversal of *ras*-mediated transformation and tumorigenesis of cloned rat embryo fibroblasts. Int. J. Cancer **55**, 841–847
20 Joshi-Barve, S., De Benedetti, A. and Rhoads, R. E, (1992) Preferential translation of heat shock mRNAs in HeLa cells deficient in protein synthesis factors eIF-4E and eIF-4γ. J. Biol. Chem. **267**, 21038–21043
21 De Benedetti, A., Joshi, B., Graff, J. R. and Zimmer, S. G. (1994) CHO cells transformed by translation factor eIF-4E display increased c-*myc* expression, but require overexpression of Max for tumorigenicity. Mol. Cell. Diff. **2**, 347–371
22 Kleijn, M., Scheper, G. C., Voorma, H. O. and Thomas, A. A. M. (1998) Regulation of translation initiation factors by signal transduction. Eur. J. Biochem. **253**, 531–544
23 Scheper, G. C., van Kollenburg, B., Hu, J., Luo, Y., Goss, D. J. and Proud, C. G. (2002) Phosphorylation of eukaryotic initiation factor 4E markedly reduces its affinity for capped mRNA. J. Biol. Chem. **277**, 3303–3309
24 Minich, W. B., Balasta, M. L., Goss, D. J. and Rhoads, R. E. (1994) Chromatographic resolution of *in vivo*-phosphorylated and nonphosphorylated translation initiation factor eIF-4E: demonstration of increased cap affinity of the phosphorylated form. Proc. Natl. Acad. Sci. U.S.A. **91**, 7668–7672
25 Joshi, B., Yan, R. and Rhoads, R. E. (1995) *In vitro* synthesis of human protein synthesis initiation factor 4γ and its localization on 43S and 48S initiation complexes. J. Biol. Chem. **269**, 2048–2055
26 Flynn, A. and Proud, C. G. (1995) Serine 209, not serine 53, is the major site of phosphorylation in initiation factor eIF-4E in serum-stimulated Chinese hamster ovary cells. J. Biol. Chem. **270**, 21684–21688
27 Marcotrigiano, J., Gingras, A.-C., Sonenberg, N. and Burley, S. K. (1997) Cocrystal structure of the messenger RNA 5′ cap-binding protein (eIF4E) bound to 7-methyl-GTP. Cell **89**, 951–961.
28 Lamphear, B. J. and Rhoads, R. E. (1990) Cap binding protein complex that restores protein synthesis in heat-shocked Ehrlich cell lysates contains highly phosphorylated eIF-4E. J. Biol. Chem. **265**, 5333–5336
29 Haghighat, A. and Sonenberg, N. (1997) eIF4G dramatically enhances the binding of eIF4E to the mRNA 5′-cap structure. J. Biol. Chem. **272**, 21677–21680
30 Rau, M., Ohlmann, T., Morley, S. J. and Pain, V. M. (1996) A re-evaluation of the cap-binding protein, eIF-4E, as a rate-limiting factor for initiation of translation in reticulocyte lysate. J. Biol. Chem. **271**, 8983–8990
31 Lachance, P. E. D., Miron, M., Raught, B., Sonenberg, N. and Lasko, P. (2002) Phosphorylation of eukaryotic translation initiation factor 4E is critical for growth. Mol. Cell. Biol. **22**, 1656–1663
32 Forman, H. J. and Kim, E. (1989) Inhibition by linoleic acid hydroperoxide of alveolar macrophage superoxide production: effect upon mitochondrial and plasma membrane potentials. Arch. Biochem. Biophys. **274**, 443–452
33 Hodis, H. N., Kramsch, D. M., Avogaro, P., Bittolo-Bon, G., Cazzolato, G., Hwang, J., Peterson, H. and Sevanian, A. (1994) Biochemical and cytotoxic characteristics of an *in vivo* circulating oxidized low density lipoprotein (LDL-). J. Lipid Res. **35**, 669–677
34 Pacifici, E. H. K., McLeod, L. L., Peterson, H. and Sevanian, A. (1994) Linoleic acid hydroperoxide-induced peroxidation of endothelial cell phospholipids and cytotoxicity. Free Rad. Biol. Med. **17**, 285–295
35 Duncan, R. and Hershey, J. W. B. (1984) Evaluation of isoelectric focusing running conditions during two-dimensional isoelectric focusing/sodium dodecyl sulfate-polyacrylamide gel electrophoresis: variation of gel patterns with changing conditions and optimized isoelectric focusing conditions. Analyt. Biochem. **138**, 144–155.

36 Rao, G. N. and Berk, B. C. (1992) Active oxygen species stimulate vascular smooth muscle cell growth and proto-oncogene expression. Circ. Res. **70**, 593–599

37 Wiese, A. G., Pacifici, R. E. and Davies, K. J. A. (1995) Transient adaptation to oxidative stress in mammalian cells. Arch. Biochem. Biophys. **318**, 231–240

38 Morley, S. J., Rau, M., Kay, J. E. and Pain, V. (1993) Increased phosphorylation of eukaryotic initiation factor 4α during early activation of T lymphocytes correlates with increased initiation factor 4F complex formation. Eur. J. Biochem. **218**, 39–48

39 Rychlik, W., Rush, J. S., Rhoads, R. E. and Waechter, C. J. (1990) Increased rate of phosphorylation-dephosphorylation of the translational initiation factor eIF-4E correlates with the induction of protein and glycoprotein biosynthesis in activated B lymphocytes. J. Biol. Chem. **265**, 19467–19471

40 Haghighat, A., Mader, S., Pause, A. and Sonenberg, N. (1995) Repression of cap-dependent translation by 4E-binding protein 1: competition with p220 for binding to eukaryotic initiation factor-4E. EMBO J. **14**, 5701–5709

41 Duncan, R. and Song, H.-J. P. (1999) Striking multiplicity of eIF4E-BP1 phosphorylated isoforms identified by 2D gel electrophoresis: regulation by heat shock. Eur. J. Biochem. **265**, 728–743

42 Gingras, A. C., Raught, B., Gygi, S. P., Niedzwiecka, A., Miron, M., Burley, S. K., Polakiewicz, R. D., Wyslouch-Cieszynska, A., Aebersold, R. and Sonenberg, N. (2001) Hierarchical phosphorylation of the translation inhibitor 4E-BP1. Genes Dev. **15**, 2852–2864

43 Sonenberg, N., Hershey, J. W. B. and Mathews, M. B. (eds). (2000). Translational Control of Gene Expression. Cold Spring Harbor Laboratory Press, Cold Spring Harbor, NY

44 McKendrick, L., Morley, S. J., Pain, V., Jagus, R. and Joshi, B. (2001) Phosphorylation of eukaryotic initiation factor 4E (eIF4E) at Ser209 is not required for protein synthesis *in vitro* and *in vivo*. Eur. J. Biochem. **268**, 5375–5385

45 Knauf, U., Tschopp, C. and Gram, H. (2001) Negative regulation of protein translation by mitogen-activated protein kinase-interacting kinases 1 and 2. Mol. Cell. Biol. **21**, 5500–5511

46 Ames, B. N., Shigenaga, M. K. and Hagen, T. M. (1993) Oxidants, antioxidants, and the degenerative diseases of aging. Proc. Natl. Acad. Sci. U.S.A. **90**, 7915–7922

47 Finkel, T. (1998) Oxygen radicals and signaling. Curr. Opin. Cell Biol. **10**, 248–253

48 Schreck, R., Albermann, K. and Bauerle, P. A. (1992) Nuclear factor κB: an oxidative stress-responsive transcription factor of eukaryotic cells (a review). Free Rad. Res. Comm. **17**, 221–237

49 Wang, X., Flynn, A., Waskiewicz, A. J., Webb, B. L. J., Vries, R. G., Baines, I. A., Cooper, J. A. and Proud, C. G. (1998) The phosphorylation of eukaryotic initiation factor eIF-4E in response to phorbol esters, cell stresses, and cytokines is mediated by distinct MAP kinase pathways. J. Biol. Chem. **273**, 9373–9377

50 Fukunaga, R. and Hunter, T. (1997) MNK1, a new MAP kinase-activated protein kinase, isolated by a novel expression screening method for identifying protein kinases. EMBO J. **16**, 1921–1933

51 Waskiewicz, A. J., Flynn, A., Proud, C. G. and Cooper, J. A. (1997) Mitogen-activated protein kinases activate the serine/threonine kinases Mnk1 and Mnk2. EMBO J. **16**, 1909–1920

52 Kennedy, I., Burdon, R. H. and Leader, D. P. (1984) Heat shock causes diverse changes in the phosphorylation of ribosomal proteins of mammalian cells. FEBS Lett. **169**, 267–273

53 Jurivich, D. A., Chung, J. and Blenis, J. (1992) Heat shock induces two distinct S6 protein kinase activities in quiescent mammalian fibroblasts. J. Cell. Physiol. **148**, 252–259

54 Scheper, G. C., Mulder, J., Kleijn, M., Voorma, H. O. and Thomas, A. A. M. (1997) Inactivation of eIF2B and phosphorylation of PHAS-I in heat-shocked rat hepatoma cells. J. Biol. Chem. **272**, 26850–26856

55 Rao, G. N. (2000) Oxidant stress stimulates phosphorylation of eIF4E without an effect on global protein synthesis in smooth muscle cells: lack of evidence for a role for H_2O_2 in angiotensin II-induced hypertrophy. J. Biol. Chem. **275**, 16993–16999

56 Larsson, R. and Cerutti, P. (1988) Oxidants induce phosphorylation of ribosomal protein S6. J. Biol. Chem. **263**, 17452–17458

Received 18 March 2002/31 July 2002; accepted 5 September 2002
Published as BJ Immediate Publication 5 September 2002, DOI 10.1042/BJ20020435